Aust. J. Phys., 1993, **46**, 773–97

Space Charge Effects in the Cavalleri Determination of Electron Diffusion Coefficients in Gases

B. S. Liley

Department of Physics, University of Waikato,
Private Bag 3105, Hamilton, New Zealand.

Abstract

A theoretical analysis shows that positive ion space charge effects can dominate the Cavalleri experiment. It is, however, confirmed that on operating in a linear regime, corresponding to normal experimental conditions, very accurate values for the electron diffusion coefficient can be obtained by extrapolating to zero X-ray pulse intensity. Both primary effects, associated with ions produced by the initiating ray pulse, and secondary effects, associated with ions produced by the RF sampling pulse, are taken into account.

1. Introduction

The Cavalleri technique provides a direct and accurate method for measuring the electron diffusion coefficient in gases (Cavalleri 1969; Huxley and Crompton 1974; Gibson *et al.* 1973). However, care must be taken to either adequately account for or avoid space charge effects associated with the positive ions which are inevitably produced in the diffusion cell (Rhymes *et al.* 1975). To date no quantitative analysis of these effects of direct relevance to the Cavalleri technique has been given, although such effects have been previously considered in relation to diffusion cooling (Biondi 1954). The object of this paper is to determine explicitly the magnitude of the ion space charge effects and thus provide a measure of the accuracy of past and subsequent experimental results.

The problem is complicated by both the experimental geometry and the basic nonlinear nature of the phenomena involved. Nevertheless, sufficiently accurate results can be obtained. In Section 2 the essential aspects of the Cavalleri experiment are briefly summarised and the number of ions present at any instant in time determined. In Section 3 exact solutions are found for three idealised diffusion cells and these solutions are used in Section 4 to validate the less exact solutions which are obtained for the actual experimental configuration. The results obtained in Section 4 are briefly discussed in Section 5.

2. The Cavalleri Experiment

The Cavalleri experimental configuration is shown in Fig. 1. A line source of electrons and ions is produced along the y-axis of a cylindrical glass diffusion cell of length $2W$ and radius R by a short X-ray pulse. For sufficiently high filling pressures ($\sim$10 kPa or greater) diffusion cooling can be ignored (Leemon

0004-9506/93/060773$05.00

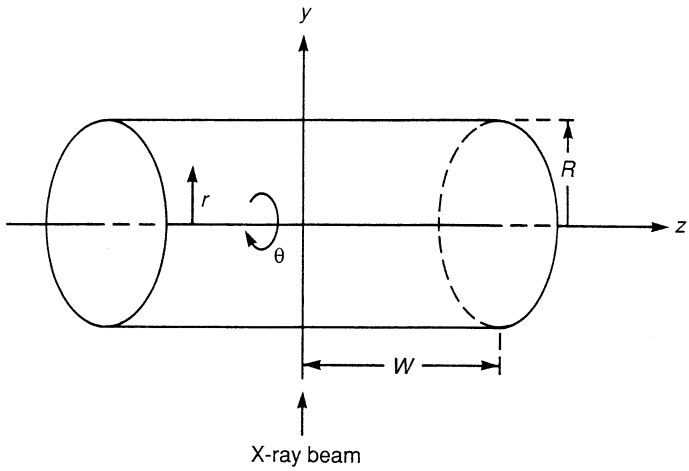

Fig. 1. Schematic diagram of the Cavalleri diffusion cell.

and Kumar 1975) and the electrons quickly thermalise, acquiring a Maxwellian distribution and a temperature equal to that of the host gas. The electrons diffuse to the walls of the cell, the positive ions remaining concentrated as a line charge during this process. In the absence of space charge effects the electron density is determined by the diffusion equation

$$\frac{\partial n}{\partial t} = D\nabla^2 n\,. \tag{1}$$

Due to the symmetry inherent in the production of the electrons the full solution of equation (1) consists of many asymmetric and radial modes. However, within a relatively short time the lowest-order mode can be expected to dominate (Huxley and Crompton 1974; Rhymes *et al.* 1975) and

$$n = n(\boldsymbol{x})\,\mathrm{e}^{-\beta^2 Dt} \equiv n(\boldsymbol{x})\,\mathrm{e}^{-t/\tau}\,, \tag{2}$$

where

$$n(\boldsymbol{x}) = n_0 \cos\left(\frac{\pi}{2}\frac{z}{W}\right) J_0\left(2{\cdot}405\,\frac{r}{R}\right), \tag{3}$$

$$\beta^2 = \left(\frac{\pi}{2}\right)^2 \frac{1}{W^2} + \left(\frac{2{\cdot}405}{R}\right)^2 \equiv \frac{1}{L^2}\,, \tag{4}$$

$$\tau \equiv \frac{1}{\beta^2 D} = \frac{L^2}{D}\,,$$

and where τ is the diffusion time and L the characteristic diffusion length of the cell.

At a sampling time t_s after the X-ray pulse, the total number of electrons in the chamber is 'determined' by the application of an RF pulse between two

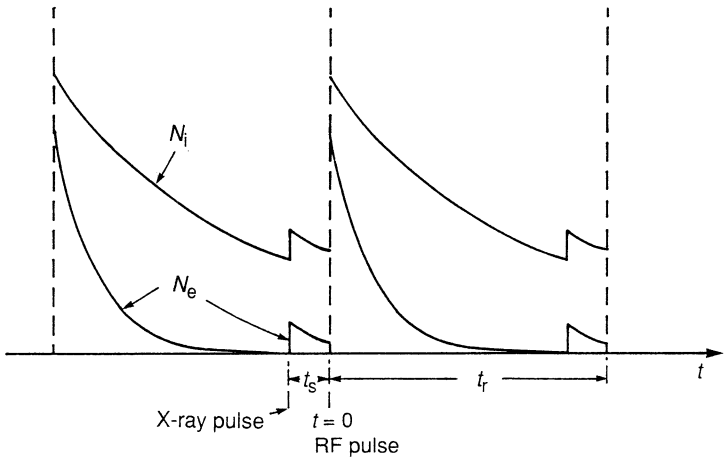

Fig. 2. Schematic diagram of the experimental cycle. Here $t = 0$ is chosen to coincide with the application of an RF pulse, while N_i and N_c are the *total* number of ions and electrons in the cell.

end plates at $z = \pm W$. Each electron present causes ionisation in its immediate vicinity, the associated light emitted providing a means of detection. Two such sampling pulses at different t_s (for two separate X-ray pulses) enable τ to be determined independently of both the actual number of electrons present and the multiplication factor involved with the RF pulse. However, in order to obtain statistically reliable results the two measurements at different t_s have to be repeated many thousands of times. Thus space charge effects not only arise from the positive ions produced by an initial X-ray pulse, but there are also cumulative effects arising from both subsequent X-ray and RF pulses. It is to be anticipated that an equilibrium state will be reached with the cycle of events being as illustrated in Fig. 2. In this figure zero time has been chosen to coincide with an RF pulse, the X-ray pulse having been applied at a time $t = -t_s$. Here N_i and N_e are the total number of ions and electrons in the cell at time t and t_r is the repetition time. If we assume that we can take $N \sim e^{-t/\tau}$, with τ a constant for both electrons and ions, then at $t = 0^-$

$$N_i(0^-) = N_x\, e^{-t_s/\tau_i} + N_i(0^+)\, e^{-t_r/\tau_i}\,,$$

$$N_e(0^-) = N_x\, e^{-t_s/\tau_e} + N_e(0^+)\, e^{-t_r/\tau_e}\,, \tag{5}$$

while at $t = 0^+$

$$N_e(0^+) = (1 + A)[N_x\, e^{-t_s/\tau_e} + N_e(0^+)\, e^{-t_r/\tau_e}]\,,$$

$$N_i(0^+) = N_i(0^-) + AN_e(0^-)\,. \tag{6}$$

In these equations $N_{ix} = N_{ex} = N_x$ is the number of electrons and ions produced by a single X-ray pulse, while A is the number of electrons and ions produced by the RF pulse for each electron present at $t = 0^-$.

Equations (5) and (6) constitute the cycle balance equations and may be immediately rearranged to give

$$N_e(0^-) = \frac{N_x\, e^{-t_s/\tau_e}}{1-(A+1)e^{-t_r/\tau_e}}, \tag{7}$$

$$N_i(0^-) = \frac{N_x}{1-e^{-t_r/\tau_i}}\left(e^{-t_s/\tau_i} + \frac{Ae^{-(t_s/\tau_e+t_r/\tau_i)}}{1-(A+1)e^{-t_r/\tau_e}}\right). \tag{8}$$

We note, in particular, the 'breakdown' condition

$$1 = (A+1)e^{-t_r/\tau_e}. \tag{9}$$

However, the experimental measuring range is such that in normal circumstances

$$t_s \sim \tau_e(\sim 10\ \mu s) \ll t_r \sim \tau_i(\sim 1\ s), \tag{10}$$

leading to

$$1 \gg (A+1)e^{-t_r/\tau_e}. \tag{11}$$

These same conditions also give

$$N_i(0^-) \approx N_i(-t_s) \equiv N_i(s;\, t_r) = N_i, \qquad -t_s < t < 0. \tag{12}$$

That is, N_i is a constant throughout the sampling time and (7) and (8) reduce to

$$N_e(0^-) = N_x\, e^{-t_s/\tau_e}, \tag{13}$$

$$N_i(s;\, t_r) = \frac{N_x}{1-e^{-t_r/\tau_i}}\left(1 + A\, e^{-(t_s/\tau_e+t_r/\tau_i)}\right). \tag{14}$$

Noting that A must be significantly greater than unity, two extremes are readily identified. If $t_r \gg \tau_i$, $N_i(s;\, t_r) \approx N_x$ and the dominant space charge effect is that associated with a positive line charge along the y-axis produced by the initiating X-ray pulse at $t = -t_s$. On the other hand, for $t_r \sim \tau_i$, not only will $N_i(s;\, t_r) \gg N_x$ but the dominant charge will be dispersed throughout the cell, being primarily that due to the RF pulse. The initial distribution of such charge for any single RF pulse will be that of the electrons at $t = 0^-$. However, at $t = -t_s$ the distribution will be that determined by the ions themselves. The problem is complicated by the fact that the ions will be subjected to their own space charge field with $N_i \sim e^{-t/\tau_i}$, $\tau_i =$ constant, being a somewhat questionable assumption. This is further discussed in Section 4.

3. Space Charge Effects

The basic equations are

$$\nabla . \boldsymbol{E} = \sum_j n_j \, e_j / \epsilon_0 \,, \tag{15}$$

$$\frac{\partial n_j}{\partial t} + \nabla . \Gamma_j = 0 \,, \tag{16}$$

$$\Gamma_j = n_j \, \mu_j \, \boldsymbol{E} - D_j \, \nabla n_j ; \qquad \frac{D_j}{\mu_j} = \frac{kT}{e_j} \,. \tag{17}$$

Both electrons ($j \equiv \mathrm{e}$) and ions ($j \equiv \mathrm{i}$) are considered. For Maxwellian velocity distributions the diffusion coefficient D is isotropic and the usual Einstein relation between D and μ, the mobility, exists. Here T is the gas temperature and k Boltzmann's constant.

Using (17) in (16) we have

$$\frac{\mathrm{d}n_j}{\mathrm{d}t_j} - D_j \, \nabla^2 n_j + \mu_j \, n_j \, \nabla . \boldsymbol{E} = 0 \,, \tag{18}$$

where $\boldsymbol{E}$ is determined by (15) and

$$\frac{\mathrm{d}n_j}{\mathrm{d}t_j} \equiv \frac{\partial n_j}{\partial t} + \mu_j \, \boldsymbol{E} . \nabla n_j \,.$$

Equation (18) has a simple physical interpretation. Referred to a frame moving with velocity $\mu_j \, \boldsymbol{E}$, particles j are dispersed (or congregated) by both diffusive and localised space charge effects (the $\nabla . \boldsymbol{E}$ term).

Noting that $\boldsymbol{E} = -\nabla \phi$, we put

$$\psi = \phi / 2kT \,, \tag{19}$$

and make the substitution

$$n_j = U_j \, \mathrm{e}^{-e_j \psi} \,. \tag{20}$$

Equations (17) and (18) then become

$$\Gamma_j = -D_j (U_j \, e_j \, \nabla \psi + \nabla U_j) \mathrm{e}^{-e_j \psi} \,, \tag{21}$$

$$\frac{1}{D_j} \frac{\partial U_j}{\partial t} - \nabla^2 U_j + b_j^2 \, U_j = 0 \,, \tag{22}$$

where

$$b_j^2 \equiv (e_j \, \nabla \psi)^2 - e_j \, \nabla^2 \psi - \frac{e_j}{D_j} \frac{\partial \psi}{\partial t} \,, \tag{23}$$

and the Poisson equation is

$$\nabla^2\psi = -\frac{1}{2kT\epsilon_0}\sum_k e_k U_k \mathrm{e}^{-e_k\psi}. \tag{24}$$

Equations (23) and (24) (three in total) are to be solved subject to appropriate initial and boundary conditions. The latter are

$$n_j = 0 \Rightarrow U_j = 0 \tag{25}$$

at the walls of the diffusion cell and

$$\Gamma_j = 0 \Rightarrow \hat{\boldsymbol{r}} \cdot \nabla U_j = -(\hat{\boldsymbol{r}} \cdot \nabla\psi) e_j U_j \tag{26}$$

at any plane or line of symmetry, $\hat{\boldsymbol{r}}$ being a unit normal to such a plane or line.

We seek solutions of the form

$$n \sim \mathrm{e}^{-\beta^2 Dt} \Rightarrow U \sim \mathrm{e}^{-\beta^2 Dt + e\psi} \equiv \mathrm{e}^{-t/\tau + e\psi}. \tag{27}$$

However, even in the absence of transients, because of the nonlinear nature of the equations such solutions only exist in the limit $n \to 0$, that is $t \to \infty$. Fortunately, the physics dominates both the geometry and the mathematics and sufficiently accurate solutions of the form (27) can be found for more realistic situations.

To define the problem explicitly, put

$$\tau = \frac{1}{\beta^2 D} = \frac{L^2}{D}\frac{1}{(\beta L)^2} \equiv \tau_0 F, \tag{28}$$

where

$$\tau_0 = \frac{L^2}{D}, \qquad F = (\beta L)^{-2}. \tag{29}$$

Here L is the characteristic diffusion length of the cell being defined such that in the absence of space charge $\tau = \tau_0$, $F = 1$. The object of the subsequent analysis is to determine βL, i.e. F, for the electrons as a function of the electron and ion concentrations in the cell. We start by considering three exact solutions.

(3a) The Planar Cell

Consider a diffusion cell consisting of two infinite plane walls separated by a distance $2W$. Ions are concentrated in an infinite plane sheet midway between the two walls (see Fig. 3). We assume that the dispersed charge is such that

$$(e_j \nabla\psi)^2 \gg |e_j \nabla^2\psi|. \tag{30}$$

This condition is a statement that the distributed charge, both electrons and ions, is small compared with the ion concentration at $z = 0$. We put

$$\boldsymbol{a}_j = e_j \nabla\psi = -e_j \frac{E}{2kT}\hat{\boldsymbol{z}} \equiv a_j \hat{\boldsymbol{z}}, \tag{31}$$

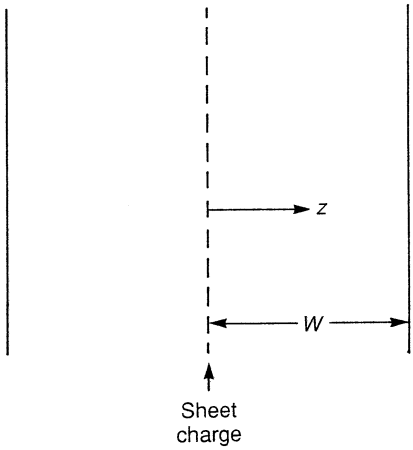

Fig. 3. Planar diffusion cell.

where, for this particular configuration and condition, E is a constant given by

$$E = \frac{N_s e_i}{2\epsilon_0}, \tag{32}$$

and where N_s is the number of ions per unit area in the sheet. Define

$$\epsilon_j = a_j W = -\frac{N_s e_i e_j W}{2\epsilon_0 kT}. \tag{33}$$

We note that a_j and hence ϵ_j is positive for electrons but negative for positive ions.

Referring now to equations (22), (25), (26) and (27), the equation to be solved is

$$\frac{d^2U_j}{dz^2} = -\alpha_j^2 U_j; \qquad \alpha_j^2 = \beta_j^2 - a_j^2, \tag{34}$$

subject to the boundary conditions

$$U_j = 0, \qquad \text{at} \quad z = W, \tag{35}$$

$$\frac{dU_j}{dz} = -a_j U_j, \quad \text{at} \quad z = 0. \tag{36}$$

We consider electrons only, for which ϵ_j and a_j are positive. On putting

$$\gamma = \alpha W \tag{37}$$

and dropping the subscript j ($\equiv$ e), the solution is

$$\epsilon \leq 1 \qquad U = A\cos\left(\gamma\frac{z}{W}\right) + B\sin\left(\gamma\frac{z}{W}\right), \tag{38}$$

$$\beta^2W^2 = \epsilon^2 + \gamma^2; \quad \frac{\gamma}{\tan\gamma} = \epsilon, \tag{39}$$

$$\gamma B = -\epsilon A, \tag{40}$$

$$\epsilon \geq 1 \qquad U = Ae^{\gamma z/W} + Be^{-\gamma z/W}, \tag{41}$$

$$\beta^2W^2 = \epsilon^2 - \gamma^2; \quad \frac{\gamma}{\tanh\gamma} = \epsilon, \tag{42}$$

$$(\gamma - \epsilon)B = (\gamma + \epsilon)A. \tag{43}$$

In particular, for $\epsilon = 1$; $\gamma = 0$, $\beta^2W^2 = \epsilon^2 = 1$ and

$$U = U_0\left(1 - \epsilon\frac{z}{W}\right) = U_0\left(1 - \frac{z}{W}\right). \tag{44}$$

In general, for this case $L = (2/\pi)W$, and on solving the eigenvalue equations (39) and (42) the factor F as defined in equation (28) can be determined, the results being given in Table 1. The origins of the analytic solutions given in this table are readily seen.

Table 1. The factor F for the planar cell (electrons only)

ϵ	γ	$F = [(2/\pi)\beta W]^{-2}$	
		Numerical value	Analytic solution
0	1·57	1	$1+2(2/\pi)^2\epsilon$
0·1	1·51	1·08	
0·2	1·43	1·18	
0·3	1·35	1·29	
0·4	1·27	1·40	
0·5	1·17	1·53	
0·6	1·05	1·68	
0·7	0·92	1·83	
0·8	0·76	2·02	
0·9	0·54	2·25	
1·0	0	2·47	$(\pi/2)^2$
1·5	1·28	4·03	
2·0	1·91	7·00	
3·0	2·98	20·5	
4·0	3·9972	$1·1\times10^2$	
5·0	4·9995	5×10^2	$(\pi^2/16)\epsilon^{-2}e^{2\epsilon}$

For $\epsilon = 0$, $\gamma = \pi/2$, hence on putting $\gamma = (\pi/2 - \delta)$ we have from equation (39)

$$\left(\frac{\pi}{2} - \delta\right) \sin\delta = \epsilon \cos\delta \,.$$

Thus for ϵ and hence δ small

$$\delta = \frac{2}{\pi}\epsilon \,,$$

$$\beta^2 W^2 = \epsilon^2 + \gamma^2 = \epsilon^2 + \left(\frac{\pi}{2}\right)^2 \left[1 - \left(\frac{2}{\pi}\right)^2 \epsilon\right]^2 .$$

On ignoring terms in ϵ^2 the analytic solution for F for small ϵ follows.

For $\epsilon > 1$ we have from (42)

$$\gamma\left(\frac{1 + \mathrm{e}^{-2\gamma}}{1 - \mathrm{e}^{-2\gamma}}\right) = \epsilon \,.$$

For ϵ large $\gamma \approx \epsilon$ and hence

$$\gamma \approx \epsilon(1 - 2\mathrm{e}^{-2\epsilon}) \,.$$

Thus

$$\beta^2 W^2 = \epsilon^2 - \gamma^2 \approx 4\epsilon^2 \mathrm{e}^{-2\epsilon} \,.$$

Finally, if we were to consider for this case the behaviour of dispersed ions (as distinct from those fixed in the sheet) we would still obtain equations (38)–(43). However, for the ions ϵ is negative and the only solution is $U_\mathrm{i} = 0$. That is, in particular, for the boundary condition (36) with $a_\mathrm{i} \neq 0$ there is no solution of the form $U_\mathrm{i} \sim \mathrm{e}^{-t/\tau_\mathrm{i}}$ with τ_i a constant. To obtain such a solution we must take $a_\mathrm{i} = 0$ at $z = 0$. That is, the ions must be completely dispersed. We return to this problem in Section 4.

(3b) The Infinite Symmetric Cylinder

Referring to Fig. 1 we take $W = \pm\infty$ and let there be a uniform positive ion line charge in the z, rather than the y, direction. Referring to (22), (23), (25) and (26), the equation to be solved is

$$\frac{\mathrm{d}^2 U}{\mathrm{d}r^2} + \frac{1}{r}\frac{\mathrm{d}U}{\mathrm{d}r} + (\beta^2 - a^2)U = 0 \,, \tag{45}$$

subject to the boundary conditions

$$U = 0 \,, \qquad r = R \,, \tag{46}$$

$$\frac{\mathrm{d}U}{\mathrm{d}r} = -aU \,, \qquad r = 0 \,. \tag{47}$$

For this case

$$\boldsymbol{a}_j = e_j \nabla\psi = -\frac{e_j E}{2kT}\hat{\boldsymbol{r}} \equiv a_j \hat{\boldsymbol{r}}\,,$$

where $E = N_l e_\mathrm{i}/2\pi r\epsilon_0$, with N_l being the number of ions per unit length. We define

$$\nu_j = -\frac{N_l e_\mathrm{i} e_j}{4\pi kT\epsilon_0} \Rightarrow a_j = \frac{\nu_j}{r}\,, \tag{48}$$

whence (45) is simply an ordinary Bessel equation of order ν.

Obviously ϵ and ν are similar dimensionless parameters. In fact on defining an equivalent mean space density n_i^0 by $N_\mathrm{s} W = 2n_\mathrm{i}^0 L^2$ and $N_l = \pi n_\mathrm{i}^0 L^2$, then

$$\epsilon = 2\left(\frac{L}{2h_\mathrm{i}}\right)^2, \qquad \nu = \left(\frac{L}{2h_\mathrm{i}}\right)^2, \tag{49}$$

where the ion Debye length is

$$h_\mathrm{i}^2 = kT/n_\mathrm{i}^0\,\epsilon_0\,. \tag{50}$$

The factor of 2 for the planar case arises from the fact that there are two sides to the cell. As will be seen in the next section (49) and (50) constitute a very important observation.

Returning to equation (45), with a given by (48), the solution for electrons is $(0 < \nu < 1)$

$$U = AJ_\nu(\beta r) + BJ_{-\nu}(\beta r) \tag{51}$$

with, in particular,

$$\frac{\mathrm{d}U}{\mathrm{d}r} = -\frac{\nu}{r}U\,, \qquad \text{at} \quad r = 0\,. \tag{52}$$

But, for $\beta r \equiv x$, for any Bessel function

$$J_n' = nx^{-1}J_n - J_{n+1}\,, \qquad J_n' \equiv \frac{\mathrm{d}J_n}{\mathrm{d}x}\,,$$
$$J_n \sim x\,, \qquad x \to 0\,,$$

and the boundary condition (52) gives $A = 0$. Thus

$$U = BJ_{-\nu}(\beta r)\,. \tag{53}$$

Equation (53) is also a solution for $\nu = 0$, that is, no space charge, and we have in particular for $\nu = 0$ and $U = 0$ at $r = R$,

$$\beta R = 2{\cdot}405 \Rightarrow L = R/2{\cdot}405\,.$$

Thus the factor F of equation (29) is simply $F = (2{\cdot}405/\beta R)^2$, with the βR being the roots of

$$J_{-\nu}(\beta R) = 0\,. \tag{54}$$

The results are given in Table 2 and presented graphically in Fig. 4. For comparison the planar case is also shown in the same figure.

Table 2. The factor F for the cylindrically symmetric cell (electrons only)

ν	βR	$F = (2{\cdot}405/\beta R)^2$	
		Numerical value	'Analytic' approximation
0	2·405	1	$1 + 2(\pi/4{\cdot}81)\nu = 1 + 1{\cdot}3\nu$
0·1	2·2486	1·14	
0·2	2·0883	1·30	
0·3	1·9228	1·56	
0·4	1·7509	1·88	
0·5	1·5708	2·34	$[(2/\pi)2{\cdot}405]^2$

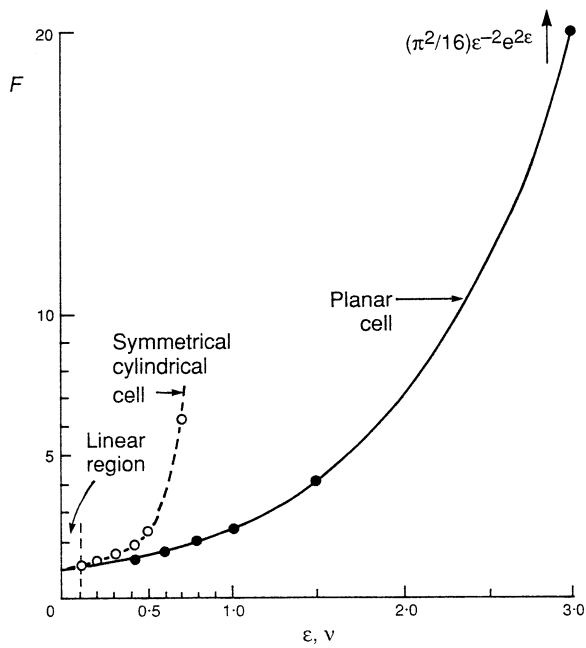

Fig. 4. The factor $F \equiv \tau_c/\tau_{c0}$ versus space charge parameters for both planar (ϵ) and cylindrically symmetric (ν) cells. Exact values are given in Tables 1 and 2.

The roots of (54) have been taken from Janke–Emde–Lösch (1960). Unfortunately, values of $\nu > 0{\cdot}5$ are not recorded but this is of no great consequence, the rapid increase of F with ν for $\nu > 0{\cdot}5$ being obvious. Again for $\nu > 1$ real roots of (54) may not exist and as in the planar case a different solution should be

found. The 'analytic' approximation given in Table 2 for $\nu \leq 0{\cdot}1$ is accurate to within 1%.

(3c) The Finite Symmetric Cylinder

Take now W to be finite and assume as before (equation 30) that space charge effects associated with dispersed charge can be ignored. Then in general for the symmetric case

$$\boldsymbol{a} = a_r\,\hat{\boldsymbol{r}} + a_z\,\hat{\boldsymbol{z}} \Rightarrow \alpha^2 = a_r^2 + a_z^2\,,$$

and from (22) the equation to be solved is

$$\frac{\partial^2 U}{\partial r^2} + \frac{1}{r}\frac{\partial U}{\partial r} - a_r^2 U + \frac{\partial^2 U}{\partial z^2} - a_z^2 U = -\beta^2 U\,, \tag{55}$$

subject to

$$\frac{\partial U}{\partial r} = -a_r U\,; \qquad r = 0\,, \tag{56}$$

$$\frac{\partial U}{\partial z} = -a_z U\,; \qquad z = 0\,, \tag{57}$$

$$U = 0\,; \qquad r = R\,, \quad z = W\,. \tag{58}$$

In the absence of space charge a solution of (55) determines L, this being, as already noted (equation 4), given by

$$\frac{1}{L^2} = \left(\frac{\pi}{2}\right)^2 \frac{1}{W^2} + \left(\frac{2{\cdot}405}{R}\right)^2. \tag{59}$$

Again, in general, we have

$$F = (\beta L)^{-2}\,. \tag{60}$$

Put now

$$\beta^2 = \beta_r^2 + \beta_z^2\,, \tag{61}$$

and define

$$F_r = \left(\frac{2{\cdot}405}{\beta_r R}\right)^2, \qquad F_z = \left(\frac{\pi}{2\beta_z W}\right)^2, \tag{62}$$

then we have

$$\frac{1}{F} = \left[\left(\frac{2\cdot 405}{R}\right)^2 \frac{1}{F_r} + \left(\frac{\pi}{2W}\right)^2 \frac{1}{F_z}\right] L^2 . \tag{63}$$

This is a general expression but for it to be of value we must be able to determine β_r and β_z separately. For a_r and a_z functions of r or z only, or a_r and a_z functions of r only and z only respectively, separation of variables is possible and solutions of the type already discussed are readily obtained.

Of special interest is the case of an infinite line of positive charge along the z-axis ($r = 0$) plus an infinite plane sheet of positive charge in the xy plane (cf. Fig. 1). For this case F_r and F_z are as given in Tables 1 and 2. If now, in particular, the xy sheet charge is zero, then

$$F_z = 1 . \tag{64}$$

Then as the line charge is increased from zero to some relatively large value, F_r will rapidly increase and F will tend to a saturation value

$$F_{\text{sat}} = \left(\frac{2}{\pi} W\right)^2 \Big/ L^2 = \left(\frac{4\cdot 81}{\pi}\right)^2 \frac{W^2}{R^2} + 1 . \tag{65}$$

or for $R = W$

$$F_{\text{sat}} = 3\cdot 34 . \tag{66}$$

This result is of considerable interest for the actual Cavalleri configuration.

4. The Actual Experimental Configuration

The actual experimental configuration differs considerably from those discussed in the preceding section. In the first place, referring to Fig. 1, any line charge will be along the y-axis instead of the symmetry (z) axis. Again depending on the repetition time, t_r, much of the associated space charge will be distributed throughout the cell rather than concentrated in a line or on a plane. The result is that no exact solutions comparable with those found in Section 3 are possible. However, using the reults of Section 3, approximations of sufficient accuracy can be found. Referring to Section 2 we consider two cases, $N_{\text{i}}(s;\, t_{\text{r}}) = N_{\text{x}}$ and $N_{\text{i}}(s;\, t_{\text{r}}) \gg N_{\text{x}}$.

(4a) The Case $N_{\text{i}}(s;\, t_{\text{r}}) = N_{\text{x}}$

For this case the charge is concentrated along the y-axis and condition (30) is still satisfied. The basic problem is readily identified. Referring to Fig. 5 and ignoring end effects

$$\boldsymbol{E} = \frac{N_l\, e_{\text{i}}}{2\pi R \epsilon_0}\, \hat{\boldsymbol{R}}, \qquad \psi = -\frac{N_l\, e_{\text{i}}}{4\pi k T \epsilon_0} \ln R , \tag{67}$$

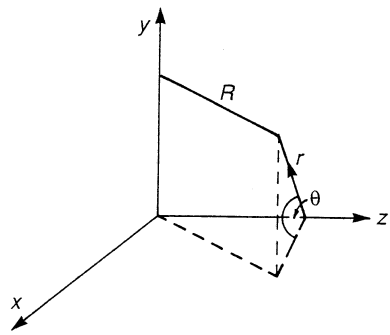

Fig. 5. Radial variable R as a function of the cell variables r, θ, z.

where

$$R^2 = z^2 + x^2 = z^2 + r^2 \sin^2 \theta \,. \tag{68}$$

For the r, θ, z coordinate system of Fig. 5

$$\boldsymbol{a}_j = e_j \nabla \psi = -\frac{N_l \, e_i \, e_j}{4\pi k T \epsilon_0} \frac{1}{R^2} \left(r \sin^2 \theta \, \hat{\boldsymbol{r}} + r \cos \theta \, \sin \theta \, \hat{\boldsymbol{\theta}} + z \, \hat{\boldsymbol{z}} \right),$$

$$a_j^2 = \left(\frac{N_l \, e^2}{4\pi k T \epsilon_0} \right)^2 \frac{1}{z^2 + r^2 \sin^2 \theta} \,.$$

It follows that for a_j other than zero, solutions involving separation of variables do not exist.

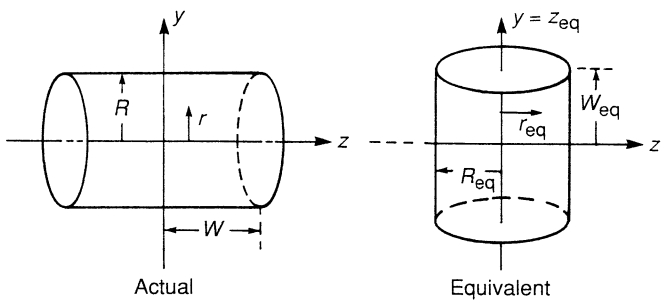

Fig. 6. Actual and equivalent Cavalleri configurations for $N_i(s; t_r) = N_x$.

However, if we think of y and R as being the variables with $y \equiv z = z_{eq}$, $R \equiv r = r_{eq}$, we can consider the equivalent system shown in Fig. 6. For both the actual and equivalent system the line charge is along the y-axis and

$$E_y = a_y = a_{z_{eq}} = 0 \,. \tag{69}$$

From the preceding section, equation (63), we immediately have

$$\frac{1}{F_{\rm eq}} = \left[\left(\frac{4\cdot 81}{\pi}\,\frac{W_{\rm eq}}{R_{\rm eq}}\right)^2 \frac{1}{F_R} + \frac{1}{F_y}\right] \Big/ \left[\left(\frac{4\cdot 81}{\pi}\,\frac{W_{\rm eq}}{R_{\rm eq}}\right)^2 + 1\right], \tag{70}$$

with

$$F_y = 1 \tag{71}$$

and $F_{\rm R}$ given by Table 2. Obviously we wish to determine the ratio $W_{\rm eq}/R_{\rm eq}$ such that for the real system $F = F_{\rm eq}$.

For exact equivalence between the two systems we postulate the following conditions.

(i) Since we must have $\tau_0 = \tau_{0_{\rm eq}}$, then $L_{\rm eq} = L$. That is, from equation (4)

$$\frac{1}{W_{\rm eq}^2}\left[\left(\frac{4\cdot 81}{\pi}\,\frac{W_{\rm eq}}{R_{\rm eq}}\right)^2 + 1\right] = \frac{1}{W^2}\left[\left(\frac{4\cdot 81}{\pi}\,\frac{W}{R}\right)^2 + 1\right]. \tag{72}$$

(ii) As already implied (Section 3*b*, also see next subsection) the basic scaling parameter is $L/h_{\rm i}$; hence

$$n_{\rm i}^0 = n_{\rm i_{eq}}^0 \Rightarrow \frac{2RN_l}{2\pi R^2 W} = \frac{2W_{\rm eq}\,N_{l_{\rm eq}}}{2\pi R_{\rm eq}^2\,W_{\rm eq}}. \tag{73}$$

(iii) But in addition to (ii) we would expect the basic space charge parameter to be ν and that this should be the same for both systems, giving

$$N_l = N_{l_{\rm eq}}.$$

From (ii) it follows that we must have

$$RW = R_{\rm eq}^2. \tag{74}$$

Equations (72) and (74) now give

$$\left(\frac{4\cdot 81}{\pi}\,\frac{W_{\rm eq}}{R_{\rm eq}}\right)^2 = \left[\frac{W}{R} + \frac{R}{W}\left(\frac{\pi}{4\cdot 81}\right)^2 - 1\right]^{-1}. \tag{75}$$

For $W/R = 1$ this gives $W_{\rm eq}/R_{\rm eq} = 1$ and

$$F = F_{\rm eq} = \frac{3\cdot 34}{2\cdot 34/F_R + 1}. \tag{76}$$

The exact appropriateness of conditions (i)–(iii) is uncertain. However, the result (76) is consistent with a physical interpretation of the behaviour of F. In

particular, because of (69), and hence (71), we expect F to approach a saturation value, the electrons being restricted in the z but not the y direction by the space charge fields. Again for

$$\frac{W}{R} \gg 1 \quad \text{and} \quad \frac{W}{R} \ll 1\,, \tag{77}$$

equation (85) gives $W_{\text{eq}}/R_{\text{eq}} \ll 1$ and hence

$$F = F_{\text{eq}} \approx F_y = 1\,. \tag{78}$$

At first sight this appears to be an inappropriate result, but on reflection it is also consistent with our physical expectations. Conditions (77) are simply a measure of the relative physical scale of the system and if satisfied, the charge along the y-axis will appear as little more than a minor perturbation to the system as a whole.

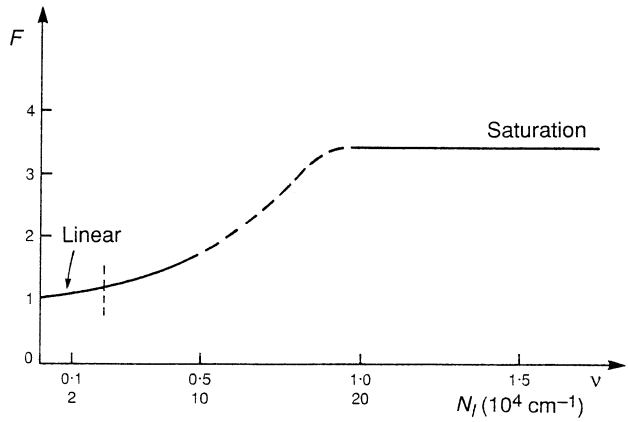

Fig. 7. Factor F versus ν and N_l (line density) for the Cavalleri experiment for $N_{\text{i}}(s;\, t_{\text{r}}) = N_{\text{x}}$.

From (76) the saturation value of F is 3·34, being within 10% of this value for $F \approx 20$. Using the values of F_{R} given in Table 2, for $R = W$ the values of F can be determined and are given in Fig. 7. The corresponding values for N_l have been deduced from (48), with $N_l = 1{\cdot}8 \times 10^5 \nu$ (cm^{-1}); $T = 300$ K.

An approximation for the linear region is readily obtained. On putting $F_{\text{R}} = 1 + \delta F_{\text{R}}$ in (76), we have

$$F = (1 + \delta F_R)\left(1 - \frac{1}{3{\cdot}34}\,\delta F_R\right) \approx 1 + \frac{2{\cdot}34}{3{\cdot}34}\,\delta F_R\,,$$

which from Table 2 is

$$\begin{aligned} F &\approx 1 + 0{\cdot}95\nu && \nu < 0{\cdot}1 \\ &= 1 + 0{\cdot}5 N_l \times 10^{-5} && (N_l \text{ in cm}^{-1})\,. \end{aligned} \tag{79}$$

We note from Fig. 7 that the major departures from linearity occur in the range $10^5 < N_l < 2 \times 10^5\ \mathrm{cm}^{-1}$, while the curve is linear to within 1% for $N_l < 4 \times 10^4\ \mathrm{cm}^{-1}$. In practice N_l is determined by the intensity I of the X-ray beam and the actual value is unknown. This is of no consequence since, provided the linear part of the F curve is found, an extrapolation for $I \to 0$ will give an extremely accurate value for τ_0. Because of this the accuracy of the preceding analysis is relatively unimportant. On the other hand, it is extremely important to ensure that the operating conditions do not correspond to the saturation level. For this region the value of F given is at best an approximation, while the apparent independence of F on I could lead to the false conclusion that space effects are insignificant. Of course it is possible that the finite length of the line charge could lead to an E_y and thus obscure the existence of a true saturation level. This however would only lead to further confusion and thus this region of the F–ν curve should be avoided.

As already noted in Section 3, other nonlinear effects could arise from the space charge field of the electrons themselves. The mean electron density at the sampling time t_s is given by

$$n_\mathrm{e} = \frac{N_l\, 2R}{2\pi R^2 W}\, \mathrm{e}^{-t_\mathrm{s}/\tau}\,. \tag{80}$$

Referring now to equations (22), (23) and (24) we have

$$\nabla^2 U_\mathrm{e} + [\beta^2(1 + e\psi_\mathrm{e}) - (e\nabla\psi)^2 - e\nabla^2\psi]U_\mathrm{e} = 0\,, \tag{81}$$

where for this case of $N_\mathrm{i}(s;\, t_\mathrm{r}) = N_\mathrm{x}$

$$\nabla^2\psi \equiv \nabla^2\psi_\mathrm{e} = \frac{e}{2kT\epsilon_0}\, U_\mathrm{e}\, \mathrm{e}^{e\psi}\,; \qquad e = |e_\mathrm{e}|\,, \tag{82}$$

and we have put

$$\frac{1}{D_\mathrm{e}}\,\frac{\partial U_\mathrm{e}}{\partial t} = -\beta^2 U_\mathrm{e}\,, \qquad \frac{1}{D_\mathrm{e}}\,\frac{\partial \psi}{\partial t} = \frac{1}{D_\mathrm{e}}\,\frac{\partial \psi_\mathrm{e}}{\partial t} = -\beta^2\psi_\mathrm{e}\,. \tag{83}$$

For β^2 to be a constant the terms in the coefficient of U_e in (81) must be independent of time. That is, the terms involving ψ_e must be negligible. A simple criterion ensuring this is

$$\beta^2 \gg e\nabla^2\psi \Rightarrow 1 \gg \frac{n_\mathrm{e}\, e^2}{2kT\epsilon_0}\, L^2\,, \tag{84}$$

or from (80)

$$\frac{N_l\, e^2}{4\pi kT\epsilon_0}\left(\frac{2L^2}{RW}\right)\mathrm{e}^{-t_\mathrm{s}/\tau} \ll 1\,. \tag{85}$$

From (48) and (4) for $R = W$ this reduces to

$$0{\cdot}24\nu\,\mathrm{e}^{-t_\mathrm{s}/\tau} \ll 1\,. \tag{86}$$

We take as a measure of t_s and τ $0{\cdot}24\mathrm{e}^{-t_\mathrm{s}/\tau} = 0{\cdot}1$, giving $\nu \ll 10$. Alternatively, for a 1% error in β^2, and hence τ, we require $\nu < 0{\cdot}1$, which corresponds to

$$N_l < 2 \times 10^4\ \mathrm{cm}^{-1}\,. \tag{87}$$

(4b) The Case $N_\mathrm{i}(s;\, t_\mathrm{r}) > N_\mathrm{x}$

From equation (14) we have

$$N_\mathrm{i}(s;\, t_\mathrm{r}) = \frac{N_\mathrm{x}}{1 - \mathrm{e}^{-t_\mathrm{r}/\tau_\mathrm{i}}}\,(1 + A'\mathrm{e}^{-t_\mathrm{r}/\tau_\mathrm{i}})\,, \tag{88}$$

where

$$A' \equiv A\mathrm{e}^{-t_\mathrm{s}/\tau_\mathrm{e}}\,. \tag{89}$$

For

$$\mathrm{e}^{-t_\mathrm{r}/\tau_\mathrm{i}} \sim 1 \tag{90}$$

the distributed charge dominates the line charge. For this situation the space charge fields inhibit electron motion in all directions and no saturation effect is to be expected. In general such distributed effects may only confuse the situation and it could well be prudent to take

$$A'\mathrm{e}^{-t_\mathrm{r}/\tau_\mathrm{i}} \lesssim 0{\cdot}1 \quad \text{(say)}\,,$$

requiring

$$t_\mathrm{r} \gtrsim \tau_\mathrm{i}\,\ln 10\,A'\,. \tag{91}$$

Given τ_i and A', which may be determined from the experiment (see Appendix A), this is a relatively easy criterion to satisfy and operation on a linear part of the τ–ν (N_l or I) curve is still possible. Unfortunately the condition (91) may be too restrictive. For example, for $A' \sim 100$ and $\tau_\mathrm{i} \sim 1$ s we would require $t_\mathrm{r} \gtrsim 7$ s. This could well be too long and to reduce this by a factor of 3 (say) we would require

$$A'\mathrm{e}^{-t_\mathrm{r}/\tau_\mathrm{i}} \sim 10\,. \tag{92}$$

It is therefore necessary to look at this case in greater detail.

We note that for $N_i(s;\, t_r) \gg N_e(s)$, equations (22), (23) and (24) become

$$\nabla^2 U_e + \beta_{eq}^2 U_e = 0\,, \tag{93}$$

$$\beta_{eq}^2 = \beta^2 - (e\nabla\psi)^2 - e\nabla^2\psi\,, \tag{94}$$

$$\nabla^2\psi = -\frac{n_i\, e}{2kT\epsilon_0}\,. \tag{95}$$

Equation (93) is a linear equation with the β^2 of (94) a constant. However, in general, ψ will be a complex and unknown function of position and a solution involving separation of variables is again no longer possible. The problem is partly simplified by noting that, on ignoring completely the line charge along the y-axis (cf. Fig. 1), the boundary conditions become

$$\frac{\partial U_e}{\partial r} = 0\,, \qquad \text{at} \quad r = 0\,, \tag{96}$$

$$\frac{\partial U_e}{\partial z} = 0\,, \qquad \text{at} \quad z = 0\,. \tag{97}$$

Nevertheless, we must still approximate. If in (93) we were to assume $\beta_{eq}^2 =$ constant then a solution of this equation subject to (96) and (97) is simply

$$U_e = U_{e0} \cos\left(\frac{\pi}{2}\,\frac{z}{W}\right) J_0\left(2{\cdot}405\,\frac{r}{R}\right),$$

with

$$\beta_{eq}^2 L^2 = 1\,, \tag{98}$$

L being as given by equation (4). Furthermore we would have from (94)

$$F = (\beta L)^{-2} = [1 + (e\nabla\psi L)^2 + eL^2\nabla^2\psi]^{-1}\,. \tag{99}$$

Such a solution of course requires both $\nabla\psi$ and $\nabla^2\psi$ to be constants, which is impossible. Again if we were to take $\nabla\psi$ constant then the boundary conditions (96) and (97) would be inappropriate. However, for n_i uniform, $\nabla^2\psi$ is a constant, while from (95)

$$|\nabla\psi| \sim \frac{x}{2h_i^2\, e}\,, \qquad x < L\,,$$

h_i being the ion Debye length as previously defined. Thus assuming (99) to be formally correct we would have

$$F = \left[1 + \left(\frac{L^2}{2h_i^2}\right)^2 \left(\frac{x}{L}\right)^2 - \frac{L^2}{2h_i^2}\right]^{-1}. \tag{100}$$

It follows that for $L/h_i \ll 1$ and a uniform ion distribution, (100) is an exact result. However, in the light of the cases considered in the preceding section we can take this a stage further. On putting $x/L = \frac{1}{2}$, we have

$$F = \frac{1}{[1 - \frac{1}{2}(L^2/2h_i^2)]^2} . \tag{101}$$

Now, as already noted, this gives an accurate result for uniform n_i for small L/h_i, while the fact that it becomes infinite for

$$L/h_i = 2 \tag{102}$$

is at least qualitatively, if not quantitatively, quite consistent with the exact solutions obtained in the preceding section. We therefore take (101) as being an adequate solution to the problem. [For $h_i < L/2$, F remains infinite, the electron 'boundary' effectively contracting, that is, L decreases, so that (102) is always satisfied.]

Inserting numbers, equation (101) is

$$F = \left(1 - \frac{N}{R}\,10^{-6}\right)^{-2} , \tag{103}$$

where N is the total number of ions in the cell and R is the radius in cm. [The numerical factor, 10^{-6}, corresponds to $R = W$, $T = 300$ K. For other cases it should be multiplied by $(W/R)(300/T)$.]

Alternatively, using (88) we have

$$\tau_e = \tau_{e0} \Big/ \left[1 - \frac{10^{-6} N_x (1 + A' e^{-t_r/\tau_i})}{R(1 - e^{-t_r/\tau_i})}\right]^2 , \tag{104}$$

with

$$A' = A e^{-t_s/\tau_e} . \tag{105}$$

For $t_r/\tau_i \gg 1$ this gives, in a linear approximation,

$$F = \tau_e/\tau_{e0} = 1 + 0{\cdot}4 N_l \times 10^{-5} , \tag{106}$$

where N_l is the equivalent line density per cm defined by $2R N_l = N = N_x$.

The agreement between (106) and (79) is remarkably good, giving credence to both results. More importantly, this agreement implies that (103) and (104) are adequate approximations irrespective of the ion distribution. It is important to appreciate fully, however, that they are by no means exact. For example, referring to (104), due to self space charge effects τ_i will be a function of all other variables N_x, A, t_r and t_s. It is to be expected that it will vary from its value, τ_{i0}, in the absence of space charge to its ambipolar value, $\tau_{i0}/2$, as $\tau_e \to \infty$. Of course τ_e will never actually become infinite, tending instead to τ_i.

In general equation (104) is the cycle balance equation and as such, because of (105), is a complex equation for τ_e. The dependence of τ_e on other parameters is given more explicitly in the alternative form

$$b = (1 - x^{\frac{1}{2}})e^{\alpha x}, \tag{107}$$

with

$$x = \frac{\tau_{e0}}{\tau_e}, \qquad \alpha = \frac{t_s}{\tau_{e0}},$$

$$b = \frac{10^{-6}}{R} N_x A \frac{e^{-t_r/\tau_i}}{1 - e^{-t_r/\tau_i}} a,$$

$$a = 1 + \frac{1}{A} e^{\alpha x} e^{t_r/\tau_i}.$$

In this form it is possible to identify two extreme cases:

(i)
$$\frac{1}{A} e^{\alpha x} e^{t_r/\tau_i} \gg 1, \tag{108}$$

for which equation (107) reduces to

$$\frac{10^{-6}}{R} N_x \frac{1}{1 - e^{-t_r/\tau_i}} = 1 - x^{\frac{1}{2}}. \tag{109}$$

This corresponds to both the line and distributed charge produced by the X-ray pulse being dominant. Since (108) will inevitably require $t_r \gg \tau_i$, this case has already been considered in equations (106), (79) and (91).

(ii)
$$\frac{1}{A} e^{\alpha x} e^{t_r/\tau_i} \ll 1 \Rightarrow a = 1. \tag{110}$$

This corresponds to the positive ion charge produced by the RF pulse being dominant. For this case (107) exhibits extremely interesting behaviour as a function of α, this being discussed in Appendix B.

In general in all cases the experimental observations are made in the linear region of the τ_e–N_x (i.e. I) curve in the neighbourhood of $x = 1$. Here τ_{e0} is determined by extrapolation as $I \to 0$. Using previous estimates of N_l [cf. equations (106) and (79)] this region corresponds to

$$0 < b < 0{\cdot}04. \tag{111}$$

For both the extreme cases considered here operation within these limits gives

$$\frac{\tau_e}{\tau_{e0}} = 1 + \gamma N_l, \tag{112}$$

where for the first case, from equation (106),

$$\gamma = 0{\cdot}4 \times 10^{-5} = \text{constant}, \tag{113}$$

while for the second case (see Appendix B)

$$\gamma = \frac{4 \times 10^{-6} A \, e^{-\alpha} \, e^{-t_r/\tau_i}}{1 - e^{-t_r/\tau_i}} . \tag{114}$$

Implicitly for this case e^{-t_r/τ_i} is of the order of unity, and the sensitivity of γ to A, t_r, α $(=t_s/\tau_{e0})$ and, in particular, τ_i makes operation under conditions corresponding to (110) somewhat questionable.

5. Discussion

The results obtained in this analysis emphasise not only the importance of, but the dominance of space charge effects in the Cavalleri experiment. To achieve accurate results, it is essential to operate in a regime in which the electron diffusion time is clearly dependent on the positive ion line density produced by the X-ray pulse, that is linearly dependent on the X-ray intensity I. In this regime accurate values for τ_{e0} can be obtained by extrapolating the τ_e–I curve to $I = 0$. An approximate relationship for this region is

$$\tau_e = \tau_{e0}(1 + 0{\cdot}5 N_l \times 10^{-5}) ; \qquad N_l < 2 \times 10^4 \text{ cm}^{-1} ,$$

N_l being the positive ion line density per cm. In the work of Rhymes *et al.* (1975, Fig. 1) such a linear plot is given for neon at 13·38 kPa. In terms of a relative density n_0 the equation is

$$\tau_e = \tau_{e0}(1 + 0{\cdot}04 n_0) .$$

Comparison with the preceding equation gives

$$n_0 = 1 \equiv N_l = 8 \times 10^3 \text{ cm}^{-1} ,$$

a value well within the linear limits.

For a guaranteed linear dependence on I, a basic requirement is for the repetition time t_r to be such that

$$t_r \gtrsim \tau_i [1 + \ln(A e^{-t_s/\tau_e})] , \tag{115}$$

where A is the RF pulse amplification factor, t_s the sampling time and $\tau_e \approx \tau_{e0}$. For $A e^{-t_s/\tau_e} \sim 100$ this gives $t_r \sim 7\tau_i$. Shorter repetition times are desirable. The analysis indicates that a linear dependence on N_l as such is still possible for such times but that there is a sensitivity to t_s, A, t_r and in particular τ_i, the ion containment time, which could lead to nonlinear behaviour. Such behaviour might, however, be minimised by the experimental procedures, and somewhat lower values of t_r than that given by (115) could possibly be achieved.

Acknowledgment

The author thanks Dr R. W. Crompton for suggesting this problem and for his comments.

References

Biondi, M. A. (1954). *Phys. Rev.* **93**, 1136.
Cavalleri, G. (1969). *Phys. Rev.* **179**, 186.
Gibson, D. K., Crompton, R. W., and Cavalleri, G. (1973). *J. Phys.* B **6**, 1118.
Huxley, L. G. H., and Crompton, R. W. (1974). 'The Diffusion and Drift of Electrons in Gases' (Wiley: New York).
Jahnke–Emde–Lösch (1960). 'Tables of Higher Functions' (McGraw–Hill: New York).
Leemon, H. I., and Kumar, K. (1975). *Aust. J. Phys.* **28**, 25.
Rhymes, T., Crompton, R. W., and Cavalleri, G. (1975). *Phys. Rev.* A **12**, 776.

Appendix A

The basic equations are

$$R \times 10^6(1 - x^{\frac{1}{2}}) = N(s; t_r) = \frac{N_x}{1 - e^{-t_r/\tau_i}} (1 + A e^{-\alpha x} e^{-t_r/\tau_i}) . \qquad \text{(A1)}$$

The first in this set is the space charge equation and the second the cycle balance equation. Although these equations are only approximations to the real case, they can nevertheless be regarded as exact in the sense that we wish to determine the unknowns N_x, τ_{e0}, A and τ_i by fitting such functions to experimentally determined curves. In particular, equation (104) implies that τ_e versus t_r curves for A and t_s constant will be of the form shown in Fig. 8. [This is in agreement with the observations of Rhymes *et al.* (1975, Fig. 2).] Such curves could be fitted by the functions (A1) in several ways. We only discuss one.

Equations (A1) may be rearranged to give

$$h = \frac{C - N_x}{C + \beta N_x A} ,$$

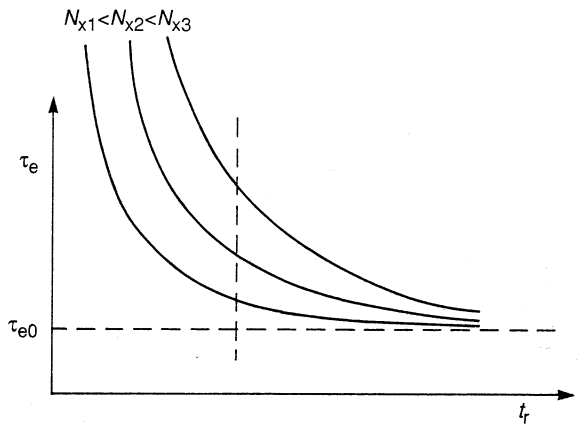

Fig. 8. Schematic curves of τ_e versus t_r for different N_x (A and t_s are held constant.)

where

$$h = e^{-t_r/\tau_i}, \qquad C = R \times 10^6(1 - x^{\frac{1}{2}}),$$

$$\beta = e^{-\alpha x}; \quad \alpha x = t_s/\tau_e.$$

On decreasing N_x, that is I, the minimum value of $\tau_e = \tau_{e0}$ can be found. Thus for given t_r and t_s, C and β are known as a function of N_x, that is I, while h is a constant. Thus

$$h = \frac{C_1 - N_{x1}}{C_1 + \beta_1 N_{x1} A} = \frac{C_2 - N_{x2}}{C_2 + \beta_2 N_{x2} A} = \frac{C_3 - N_{x3}}{C_3 + \beta_3 N_{x3} A}. \tag{A2}$$

But

$$\frac{N_{x2}}{N_{x1}} = \frac{I_2}{I_1} = \rho_2, \qquad \frac{N_{x3}}{N_{x1}} = \frac{I_3}{I_1} = \rho_3,$$

with ρ_2 and ρ_3 being known. Thus within equations (A2) there are two equations which enable A and N_{x1} to be determined, while the remaining equation determines h and hence τ_i.

Appendix B

Consider the function [equation (107)]

$$b = (1 - x^{\frac{1}{2}})e^{\alpha x}; \tag{B1}$$

we are interested in the domain

$$0 \leq x \leq 1.$$

We note that

(i) $\quad x = 1, \ b = 0; \qquad x = 1, \ b = 1,$

(ii) $$\frac{db}{dx} = \left(- \frac{1}{2x^{\frac{1}{2}}} + \alpha(1 - x^{\frac{1}{2}}) \right) e^{\alpha x},$$

giving $db/dx = -\infty$, $b = 1$ and $db/dx = -e^{\alpha}/2$, $b = 0$.

We note, in particular, that for α $(= t_s/\tau_{e0}) > 2$, equation (B1) exhibits hysteresis type behaviour with maxima and minima occurring at

$$x_{max} = \tfrac{1}{4}\left(1 + \sqrt{1 - \frac{2}{\alpha}}\right)^2; \qquad b_{max} = \tfrac{1}{2}\left(1 - \sqrt{1 - \frac{2}{\alpha}}\right) e^{\alpha x_{max}},$$

$$x_{min} = \tfrac{1}{4}\left(1 - \sqrt{1 - \frac{2}{\alpha}}\right)^2; \qquad b_{min} = \tfrac{1}{2}\left(1 + \sqrt{1 - \frac{2}{\alpha}}\right) e^{\alpha x_{min}}.$$

Curves for $\alpha = 0$, 1, 2, 3 and 4 are given in Fig. 9.

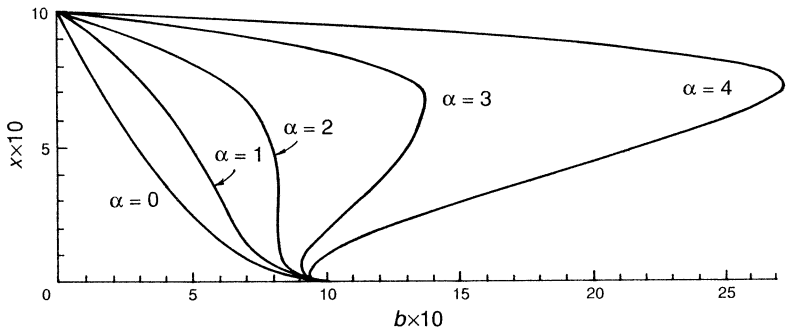

Fig. 9. The function $b = (1 - x^{\frac{1}{2}})e^{\alpha x}$ for various α.

For $A \sim 0$ the relevant curve is that for $\alpha = 0$ with [cf. equation (110)]

$$b = \frac{10^{-6}}{R} \frac{N_x}{1 - e^{-t_r/\tau_i}} . \tag{B2}$$

For A very large, corresponding to equation (110),

$$b = \frac{10^{-6}}{R} \frac{N_x A e^{-t_r/\tau_i}}{1 - e^{-t_r/\tau_i}} . \tag{B3}$$

For $\alpha > 2$ the remarkably small change in τ_e with relatively large changes in b and the possibility of more than one equilibrium state for $b > b_{min}$ is unexpected and somewhat surprising. This, however, merely reflects the ability of the system as a whole to adjust the ion concentration, and hence τ_e, to maintain the cycle. Of course not all possible equilibrium states may be stable. This has not been investigated.

A basic observation is that for given b, x increases with increasing α. That is, τ_e decreases with increasing t_s. This is not surprising since for all other parameters fixed, increasing t_s corresponds to fewer ions being produced by the RF pulse.

As noted in the main text, most experiments are conducted in the neighbourhood of $x = 1$ within the range $0 < b < 0{\cdot}04$. For A large and practical values of A and N_x this corresponds to $t_r/\tau_i \sim 3$. Again for A large from (B3) and $db/dx = -e^{\alpha}/2$ at $x = 1$, for A and t_r fixed, for $x \sim 1$ we obtain the linear relationship

$$\tau_e = \tau_{e0}(1 + 2e^{-\alpha} b) ,$$

this leading to equations (112) and (114).

Manuscript received 19 February, accepted 4 August 1993